



Basal forebrain contributes to default mode network regulation

Jaykrishnan Nair^a, Arndt-Lukas Klaassen^{a,b}, Jozsef Arato^c, Alexei L. Vyssotski^d, Michael Harvey^a, and Gregor Rainer^{a,1}

^aVisual Cognition Laboratory, Department of Medicine, University of Fribourg, 1700 Fribourg, Switzerland; ^bDepartment of Psychology, University of Fribourg, 1700 Fribourg, Switzerland; ^cDepartment of Cognitive Science, Central European University, 1051 Budapest, Hungary; and ^dInstitute of Neuroinformatics, ETH Zürich, 8057 Zürich, Switzerland

Edited by Marcus E. Raichle, Washington University in St. Louis, St. Louis, MO, and approved December 28, 2017 (received for review July 18, 2017)

The default mode network (DMN) is a collection of cortical brain regions that is active during states of rest or quiet wakefulness in humans and other mammalian species. A pertinent characteristic of the DMN is a suppression of local field potential gamma activity during cognitive task performance as well as during engagement with external sensory stimuli. Conversely, gamma activity is elevated in the DMN during rest. Here, we document that the rat basal forebrain (BF) exhibits the same pattern of responses, namely pronounced gamma oscillations during quiet wakefulness in the home cage and suppression of this activity during active exploration of an unfamiliar environment. We show that gamma oscillations are localized to the BF and that gamma-band activity in the BF has a directional influence on a hub of the rat DMN, the anterior cingulate cortex, during DMN-dominated brain states. The BF is well known as an ascending, activating, neuromodulatory system involved in wake-sleep regulation, memory formation, and regulation of sensory information processing. Our findings suggest a hitherto undocumented role of the BF as a subcortical node of the DMN, which we speculate may be important for switching between internally and externally directed brain states. We discuss potential BF projection circuits that could underlie its role in DMN regulation and highlight that certain BF nuclei may provide potential target regions for up- or down-regulation of DMN activity that might prove useful for treatment of DMN dysfunction in conditions such as epilepsy or major depressive disorder.

gamma suppression | anterior cingulate cortex | granger causality

A highly consistent finding across a wide range of functional imaging studies in humans is that a network of brain regions, referred to as the “default mode network” (DMN), increases its activity during passive mental states compared with the performance of cognitive tasks. This was initially shown in a meta-analysis of several PET studies (1), in which a distribution of brain regions broadly including the medial prefrontal, retrosplenial, and anterior cingulate cortex (ACC), as well as lateral parietal and temporal cortices, was shown to be activated when subjects were in a state of quiet restfulness. The DMN areas are thought to form a cohesive set of intrinsically coupled brain regions, such that fMRI activations in its component regions exhibit similar time courses, allowing them to be identified reliably using seed-region analysis (2–4). Activity in the DMN exhibits anti-correlation with a complementary, largely nonoverlapping, set of fronto-parietal brain areas known as the “dorsal attention network” (DAN) (5). It should be noted, however, that particular brain structures may harbor functionally heterogeneous elements and thus may contribute to multiple functions, as was shown for the ACC (6). During wakefulness, the human brain thus alternates between DAN- and DMN-dominated activation states, corresponding to effortful cognitive task performance on the one hand and quiet restfulness, introspection, and self-oriented processes on the other (7). Abnormalities in DMN processing have been linked to numerous brain disorders including epileptic seizures, clinical depression, and neurodegenerative disorders (8–10).

Following the discovery of the DMN in humans, it has subsequently been identified in other mammalian species, including

macaque monkey (11), ferret (12), and rat (13, 14). Because the DMN is an anatomically and functionally interconnected network (15), the fMRI activations in component areas tend to fluctuate in a coordinated manner even in anesthetized animals. However, some animal work has described a DMN based on awake-state data that is more in line with the studies in humans. Of particular interest is a study in chimpanzees, which demonstrated robust coherent activity in DMN structures using PET imaging (16). In this study, the PET contrast agent was injected before the animals spent time in their home cages in a state of quiet restfulness; the observed DMN activations during the PET scan indicate that the constituent brain areas were activated during the time spent in the home cage. This is important in the context of the present study, as it confirms that quiet wakefulness in the home cage is effective for activating the DMN. Direct demonstrations of the DMN activations during fMRI scans in awake animals are complicated by methodological issues such as restraint, noisy environments, and interpretational aspects (e.g., the cingulate cortex is known to be activated during anxiety) (17). Nevertheless, some evidence in awake rats suggests an emergence of a DMN-like brain state after animals have habituated to the fMRI environment (18).

A pertinent characteristic of the DMN is that brain activity in its component areas is deactivated during the performance of cognitive tasks. In humans, this deactivation has been observed not only in imaging signals but also in electrophysiological studies, including both subdural and intracranial recordings. This observation is consistent with the known coupling between

Significance

The default mode network (DMN) is suppressed during performance of externally directed cognitive tasks, and several brain disorders such as epilepsy or major depressive disorder have been linked to DMN dysregulation. Here we provide evidence suggesting that the basal forebrain (BF) may play an important role in influencing DMN activity. We show that rat BF gamma oscillations are elevated during quiet wakefulness in the home cage and are strongly suppressed during explorative behavior, similar to cortical DMN structures. Furthermore, we document directed gamma-band coherence from BF to anterior cingulate cortex (ACC), a major DMN hub. Our findings highlight a hitherto undiscovered functional influence of the BF on the ACC that may lead to therapeutic approaches for DMN disorders.

Author contributions: J.N., M.H., and G.R. designed research; J.N. and J.A. performed research; A.L.V. contributed new reagents/analytic tools; J.N., A.-L.K., M.H., and G.R. analyzed data; and J.N., M.H., and G.R. wrote the paper.

The authors declare no conflict of interest.

This article is a PNAS Direct Submission.

Published under the PNAS license.

Data deposition: The data reported in this paper are publicly available through the CRCNS - Collaborative Research in Computational Neuroscience at <https://evid.cdlib.org/id/doi:10.6080/KOMK6B2Q>.

¹To whom correspondence should be addressed. Email: gregor.rainer@unifr.ch.

This article contains supporting information online at www.pnas.org/lookup/suppl/doi:10.1073/pnas.1712431115/-DCSupplemental.

electrophysiological activity, e.g., local field potential (LFP) gamma-band oscillations, and cortical blood oxygenation level-dependent (BOLD) activation (19) and with the demonstration that pharmacological blocking of spiking activity abolishes both stimulus-evoked BOLD activity and gamma-band LFPs (20). Indeed a consistent finding related to DMN cortical deactivation during cognitive task performance is a transient suppression of the gamma band, which is time-locked to the onset of task performance and varies in amplitude in relation to task difficulty (21–24). Conversely, gamma-band activity is elevated in human DMN structures during control conditions that include quiet wakefulness, fixating one's eyes on a target, or an eyes-closed condition. This gamma-band activity is then suppressed as the DAN is activated and subjects engage with an external stimulus. In animals, it has proven difficult to reliably detect task-related deactivations in DMN structures inside the fMRI scanner, even in macaque monkeys (25–27). It is likely that animal subjects must expend considerable cognitive effort to complete the task-negative control conditions inside the fMRI scanner and that this effort does not correspond well to quiet restfulness and as a result is not associated with DMN activation (27). Outside the fMRI scanner, however, there is evidence for DMN deactivation during task performance. For example, in macaques performing a sensorimotor task, gamma oscillations are suppressed in the posterior cingulate cortex (28, 29), a constituent element of the DMN in that species (11). Similarly, sensorimotor task performance in the cat is associated with gamma deactivation from about 40 Hz upwards across many DMN structures including the ACC (30). Taken together, the task-related DMN deactivation observed in humans can be seen also in DMN regions of animal subjects, provided the control condition is of a nature that can reliably activate the DMN.

We have previously demonstrated that pronounced gamma oscillations are present in the rat basal forebrain (BF) when animals are in a wakeful state inside the home cage (31), a finding that is reminiscent of DMN activation during the task-negative behavioral states that characterize home-cage behavior (16). We therefore hypothesized that the BF may harbor a specific population of neurons that produce strong gamma oscillations when activated and at the same time are functionally coupled to the DMN. Indeed, the BF contains multiple nuclei composed of cholinergic, GABAergic, and glutamatergic corticopetal projection neurons, which are organized in segregated pools with specific projection pathways and cortical targets (32). Anatomical studies have shown that medial frontal cortical structures, including the cingulate cortex, are major targets of both cholinergic and noncholinergic BF neurons (32–34), such that in anatomical terms the BF possesses considerable connections to DMN frontal cortical structures. It has been shown that the GABAergic corticopetal BF projection, in particular, can produce robust gamma oscillations in cortical targets (35), providing a potential functional pathway by which the BF could influence DMN activation (36).

Here we provide evidence linking BF gamma oscillations to the DMN by characterizing related behaviors, demonstrating deactivation during task performance, and linking them to gamma oscillations in the cingulate cortex, a key DMN structure in the rat.

Results

We made recordings from 16 rats implanted with electrodes in the BF as well as in the visual cortex (VC) ($n = 14$) and in the ACC ($n = 8$) during awake states. Recording sites were verified in Nissl-stained sections in a subgroup of eight animals, as illustrated in Fig. 1.

Behavioral Analyses. Here we compare neural recordings from the BF, ACC, and VC obtained in three conditions: (i) exploration of an open-field arena, (ii) exploration of objects inside this arena, and (iii) home cage. Rats displayed three main behaviors in these conditions: exploration, grooming, and quiet wakefulness, as we quantified using video tracking and motion-sensor signals for a group of seven animals (SI Materials and Methods).

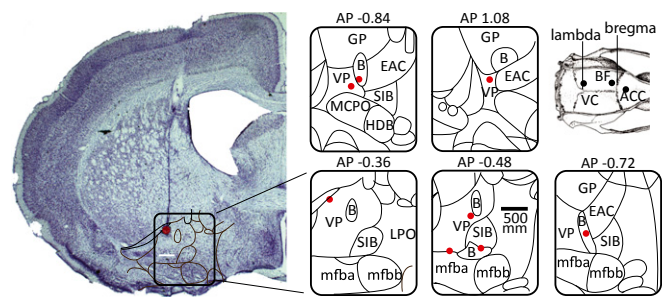


Fig. 1. Histology: A typical electrode penetration with coagulation mark. Recording sites were localized to the ventral pallidum and nucleus basalis regions of the basal forebrain. B, nucleus basalis; EAC, central extended amygdala; LPO, lateral preoptic nucleus; mfb, medial forebrain bundle; SIB, substantia innominata; VP, ventral pallidum.

In the arena, tracking analyses showed that rats spent a large majority of their time ($87.8 \pm 3.6\%$, mean \pm SEM) exploring the arena itself and objects when these were present. Only $7.6 \pm 1.7\%$ of the total time was spent grooming in this exploratory context, and animals were rarely in a state of quiet wakefulness ($1.80 \pm 0.9\%$). By contrast, rats exhibited significantly less exploratory locomotor behavior in the home cage than in the arena with or without objects (paired t tests: $P < 0.001$). Instead, they divided their time about equally (paired t test: $P > 0.1$) between states of quiet wakefulness and grooming (Fig. 2). These findings were confirmed by video monitoring based on estimating movement speed using the geometric center of the animal (mean speed: arena exploration, 8.9 ± 0.5 cm/s; object exploration, 6.9 ± 0.7 cm/s; home cage, 1.4 ± 0.4 cm/s). Locomotor behavior was greater in both exploration conditions than in the home cage (ANOVA with post hoc tests: $P < 0.01$). In addition, locomotion during arena exploration was increased compared with object exploration ($P < 0.05$), since rats tended to be stationary during object exploration.

BF Gamma Deactivation During Exploration. We observed robust BF gamma oscillations in the home-cage recordings, consistent with a previous report (31). The main finding of the present study is a striking ($35 \pm 3\%$) and highly significant (paired t test, $P < 10^{-5}$) reduction of this BF gamma activity when rats were transferred from their home cage to a novel, empty arena which they explored during a 10-min interval (Fig. 3A). BF gamma reductions were significant in all brain hemispheres ($n = 22$) when analyzed individually (unpaired t test $P < 0.01$). Thus, BF gamma was largely deactivated when rats were performing an attentionally demanding explorative task directed toward the external environment, an unexpected and surprising finding in light of the generally accepted notion that the BF is part of an arousal network contributing to attention and reward processing. Gamma oscillations are generally considered to be locally generated, but to be certain that the observed gamma activity was localized to the BF, we implanted four additional animals with bipolar electrodes (SI Materials and Methods) allowing recordings with minimal interference from surrounding areas due to volume conduction (37). Strong BF gamma activity in the home cage was also observed in these bipolar recordings, and this oscillatory activity was again strongly suppressed during arena exploration, ($24 \pm 3\%$ reduction; paired t tests: $P < 10^{-4}$).

Next we examined whether BF gamma deactivation was related to differences in locomotor behavior between arena-exploration and home-cage conditions. Specifically, we sorted 2-s LFP epochs into quartiles based on movement sensor activity. This analysis, shown in Fig. 3B, demonstrates that BF gamma activity in the arena was largely unrelated to locomotor behavior (one-way ANOVA: $P > 0.1$) and that gamma suppression during exploration remained highly significant when LFP epochs matched for movement were analyzed (e.g., the fourth and third movement quartiles for home cage and arena, respectively; one-way ANOVA:

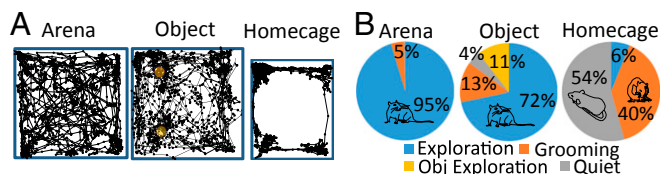


Fig. 2. Behavior analysis. (A) Schematic representation of the movement path during the behavioral conditions. Yellow circles represent objects. (B) Pie charts illustrating the occurrence of different behaviors in the three behavioral conditions.

$P < 0.001$). BF gamma activity increased with locomotor behavior in the home cage (one-way ANOVA: $P < 0.05$), was consistent over the 3 d of testing (one-way ANOVA: $P > 0.1$) (Fig. 3C), and was larger in the home cage than during either of the two arena-exploration sessions (two-way ANOVA with factors day and session and post hoc tests: $P < 10^{-4}$). In addition, gamma activity was slightly increased during the second arena-exploration session compared with the first session ($5.62 \pm 1.2\%$; post hoc test: $P < 0.01$), and there was no significant interaction between day and session number. While gamma activity was continuously suppressed in the arena, it was positively correlated with time spent in the arena ($r = 0.72$, $n = 22$, $P < 10^{-4}$) during individual exploration sessions, as shown in Fig. 3D. This reduction in gamma suppression may reflect the animal's increasing familiarity with the arena during the course of the exploration session. Nevertheless, gamma increased rapidly when the rat was transferred back to its home cage. The spectral analysis for a single-session example confirms the stationary nature of gamma in the two environments (Fig. 3E).

In the arena, rats spent a large fraction of their time exploring and only occasionally paused for some grooming ($4.6 \pm 0.3\%$ of the total time), which was associated with periods of elevated gamma in the LFP, as illustrated in Fig. 3E. These excursions of gamma power into an elevated range are described and quantified in Figs. S4 and S5. In the home cage, rats spent similar amounts of time grooming and in quiet wakefulness, so we examined the extent to which these two behavioral states were associated with gamma activity. The results, shown in Fig. 3F, indicate that gamma activity was higher during grooming than during quiet wakefulness (one-way ANOVA with post hoc tests: $P < 0.001$), but gamma activity was elevated during both quiet wakefulness and grooming compared with arena exploration ($P < 0.01$ and $P < 0.001$, respectively).

Having observed robust gamma suppression during several consecutive days of arena exploration, we next examined BF gamma oscillations during the exploration of two identical objects that were introduced into the arena following the last arena-exploration session (Fig. 4A). We found that gamma suppression was maintained during the object-exploration task, with gamma being similarly attenuated for object and empty arena exploration compared with home-cage values (one-way ANOVA: $P < 0.01$ and $P < 0.001$, respectively), and was not significantly different from the arena-exploration value ($P > 0.1$). We used manual video scoring to identify periods of object exploration during the course of the object-exploration task; results for a sample dataset are shown in Fig. 4B. This analysis illustrates that no elevation in gamma oscillations was noticeable during object exploration, suggesting that BF gamma deactivation is common to an exploratory behavioral context. This assertion is supported by a group analysis comparing BF gamma power during both empty arena and object exploration with reference values in the home cage (Fig. 4C), which illustrates highly consistent deactivation of gamma oscillations during exploration tasks (paired t tests: $P < 10^{-6}$ and $P < 10^{-5}$ for object and arena exploration, respectively).

A local contribution to the generation of a brain oscillation can be confirmed by examining the relationship of spiking activity to the oscillatory phase. We recorded 49 well-isolated BF neurons in six animals. Of these neurons, 25 exhibited significant phase locking to broadband (30–80 Hz) gamma oscillations (Hodge-

Ange circular O-test: $P < 0.01$). Preferred phase angles for all our phase-locked neurons are shown in Fig. 5A, with roughly equivalent numbers preferring the rising and falling edge of the oscillatory cycle; note that 0° corresponds to the peak of the oscillatory cycle and that four neurons were recorded under both home-cage and arena conditions. We next filtered the LFP data between 1 and 100 Hz in 10 frequency bands (1–10 Hz, 10–20 Hz, ... 90–100) and calculated the probability of a spike occurring over 25 phase angles (14.4° bins) at each band pass. Fig. 5B shows an example for two representative neurons. For both these neurons it is clear that phase locking is strongest at the higher-frequency bands (Fig. 5C), and indeed this held true for the population. We calculated a phase-locked index (PLI) as the coefficient of variation over the 25 bins at each band pass, and with this metric phase locking was found to be maximal at gamma frequencies in both the home cage and arena (one-way ANOVA, $P < 0.005$) (Fig. 5C and D). In addition, we calculated the waveform durations for our phase-locked and non-phase-locked neurons (the first negative trough to the first positive peak). Spike durations of the phase-locked neurons were significantly shorter (mean = $214 \pm 5 \mu\text{s}$) than for the non-phase-locked neurons (mean = $247 \pm 12 \mu\text{s}$; $P < 0.05$), consistent with the idea that our phase-locked units may be GABAergic fast-spiking neurons (38). Additionally, robust gamma was evident in the spike-triggered average LFP as well as in the autocorrelations of the spiking activity of individual neurons (Fig. 5E), further indicating that circuits local to the BF contribute to the gamma-band LFP oscillations observed in the present study.

Gamma Oscillations in BF Cortical Projection Targets. The robust presence of BF gamma oscillations during quiet wakefulness and grooming, coupled with their profound suppression during exploratory behaviors raises the possibility that the BF might be involved in the DMN. We explored this possibility by simultaneous recordings of the BF and ACC, an important node of the DMN. We observed that, as in the BF, gamma LFP activity was elevated in the ACC when rats were in their home cage, compared with arena exploration (paired t test: $P < 0.0$) (Fig. 6A, Left). As in the BF, gamma activity switched rapidly to an elevated state when rats were transferred to their home cage after arena exploration. This gamma enhancement did not occur in all cortical regions, as we demonstrate using paired recordings in

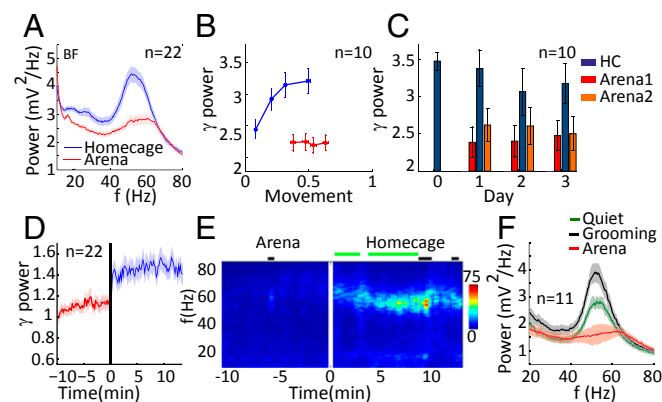


Fig. 3. BF gamma deactivation during arena exploration. (A) BF spectral power in the home cage and during arena exploration. f , frequency. (B) Movement-sensor values in quartiles plotted against gamma power for the home-cage and arena-exploration conditions. (C) Consistency of gamma power suppression over multiple days of arena exploration. HC, home cage. (D) Rapid switching of gamma power upon transfer to the home cage. The vertical line indicates the time of switching. (E) Single-session LFP spectrogram of BF activity in the arena and arena-exploration conditions. Bars above the spectrogram indicate epochs when exploratory locomotor behavior was interrupted by grooming (black bars) and quiet wakefulness (green bars). (F) Average BF gamma power for different behaviors (shaded areas represent SEM). f , frequency.

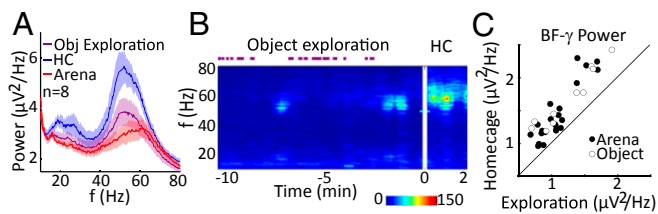


Fig. 4. BF gamma deactivation during object exploration. (A) Average LFP gamma power during object and arena exploration compared with home cage (HC) values. *f*, frequency. (B) Single-session BF LFP spectrogram during object-exploration and home-cage conditions. Purple bars above the spectrogram represent epochs of object exploration. (C) Scatter plot of BF gamma activity during arena and object exploration plotted against home-cage values across individual recordings.

the BF and VC. Thus, VC gamma activity (40–60 Hz) was unchanged between arena-exploration and home-cage environments [paired *t* test: $P > 0.1$ (Fig. 6*A*, *Right*)]. However, we did observe enhanced high gamma activity between 60 and 100 Hz during arena exploration (paired *t* test: $P < 10^{-8}$), which we attribute to previously described VC activation during locomotion (39, 40). To explore the functional coupling of the two cortical areas with the BF, we computed coherence spectra (Fig. 6*B*). We found that coherence at gamma frequencies was greater between the BF and ACC than between the BF and VC across behavioral conditions (two-way ANOVA: $P < 0.01$). Additionally, for both cortical areas, coherence with the BF was elevated in the home cage compared with the arena (two-way ANOVA: $P < 0.01$).

These results are consistent with the idea that the BF might harbor a population of neurons that generate large gamma oscillations and form part of a subcortical aspect of the DMN. To further explore the nature of BF-to-ACC communication, we performed Granger causality analyses, which can provide evidence regarding the direction of information flow between the two structures. Since BF gamma activity tended to occur in bursts, we conducted this analysis specifically during BF gamma bursts with a duration greater than 100 ms (Fig. 6*C*) and examined BF-ACC and BF-VC directional coupling in separate bivariate analyses (*SI Materials and Methods*). Consistent with our previous findings in the VC (31), directional interactions were stronger in the corticopetal than in the corticofugal direction for both the ACC and VC (two-way ANOVAs, main effects of direction: $P < 0.01$), as is consistent with the BF being a source of cortical gamma modulation (Fig. 6*C*, *Left*). However, directional interactions to the ACC were significantly larger than to the VC (two-way ANOVA, main effect of pathway: $P < 0.05$) as well as being more pronounced in the home cage than in the arena (two-way ANOVAs, main effect of location: $P < 0.016$) (Fig. 6*C*). Taken together, these findings suggest pronounced BF-to-ACC directional communication particularly when rats are in their home cage and thus are associated with behavioral states of quiet wakefulness and grooming. We further corroborated these findings by analyzing Granger causality in a subgroup of animals with electrodes implanted in the BF, VC, and ACC, permitting trivariate analyses (Fig. 6*D*). These findings illustrate BF-cortex directionality of interactions and the specificities in terms of cortical region, i.e., ACC over VC, as well as behavioral state, i.e., home cage over arena.

Taken together, our analyses support the hypothesis that the BF contains a population of neurons that (i) project to the ACC, (ii) are activated during DMN-associated behavioral states, (iii) give rise to pronounced gamma oscillations within the BF, and (iv) up-regulate cortical gamma oscillations in ACC.

Discussion

The task-related deactivation of BF gamma oscillations we describe here is counterintuitive, given that the BF is generally conceptualized as an ascending arousal system that modulates

processing in sensory cortices and contributes to mental functions more akin to the human DAN (41–44). For example, the BF modulates the response gain of single neurons in the VC as well as enhancing the sensitivity of these neurons to low-contrast visual stimuli (45–49), highlighting that the BF augments the cortical representation of sensory stimuli, consistent with some aspects of attentional modulation (50). Along related lines, BF stimulation also accelerates visual learning and up-regulates cortical visually-evoked potentials (51, 52) as well as boosting the reliability of neural signals about sensory information (53–55). Demonstrations linking BF activity to reward expectation and reward processing further implicate this brain area in goal-directed, externally focused behaviors (56, 57). Many of these BF functions are linked to cholinergic projections, which represent one of the major output pathways by which the BF can modulate cortex and other brain structures (32, 58, 59).

The present study suggests that, in addition to the functions described above that promote sensory processing and goal-directed behavior, the BF also possesses a pathway that serves a very different purpose, in that it promotes disengagement from the external environment by activating the DMN. This pathway is characterized by pronounced gamma-band activity within the BF and is functionally coupled to cortical gamma oscillations in the ACC, a major node of the DMN. We consider it likely that either the glutamatergic or the GABAergic BF projection system mediates these effects. In vitro studies have shown that both these BF populations exhibit maximum firing rates above 50 Hz and thus could participate in rhythmic firing at the gamma frequencies reported in the present study. Interestingly, the glutamatergic projection has been shown to be inhibited by cholinergic activation (60, 61), which would provide a mechanism by which the DMN is suppressed during externally directed attentional processing. However, the glutamatergic BF population does not support a pronounced projection to the DMN or even to cortex more generally. It does, however, exhibit strong projections to the ventral striatum (VS), a brain region that also exhibits pronounced gamma oscillations (62, 63), which have been shown to occur frequently in task-negative contexts as noted above (62–64). Mediated through the VS, the BF could exert control over DMN cortical areas by modulating gamma activity in the limbic cortico-striatal loop. Another possibility for mediating BF effects on DMN regulation are the GABAergic BF projections, a scenario that is supported by the fact that both parvalbumin and somatostatin GABAergic cells project strongly only to two cortical regions, namely, the ACC and retrosplenial cortex (59), both of which are major DMN nodes. Furthermore, rhythmic activation of BF parvalbumin GABAergic

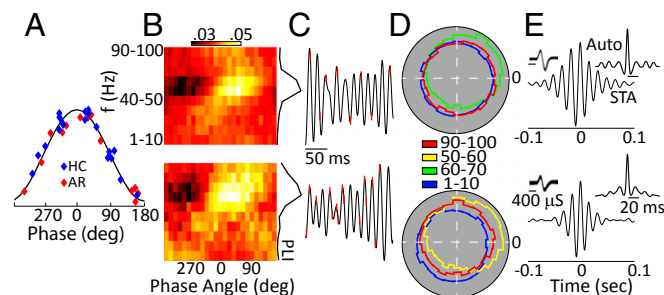


Fig. 5. BF spiking activity couples to gamma oscillations. (A) Distribution of the best phase angle for each of our phase-locked neurons for both home-cage (HC) and arena (AR) conditions. (B–E) One sample neuron recorded in the home cage (Top Row) and in the arena (Bottom Row). (B) Probability of firing in a particular 14° bin over 10 bandpass filters for the LFP data. The PLI is shown at right and is the coefficient of variance over all angles for each band pass. *f*, frequency. (C) Spike times (red hash mark) on the LFP (black solid lines). (D) Polar histograms of the phase responses at each neuron's best frequency and at the minimum and maximum band pass used. (E) Spike-triggered averages and autocorrelations (*insets*) show 1,000 waveforms for each unit. The spiking and LFP recordings analyzed here were obtained from the same electrode.

15. Stafford JM, et al. (2014) Large-scale topology and the default mode network in the mouse connectome. *Proc Natl Acad Sci USA* 111:18745–18750.
16. Rilling JK, et al. (2007) A comparison of resting-state brain activity in humans and chimpanzees. *Proc Natl Acad Sci USA* 104:17146–17151.
17. Bliss TV, Collingridge GL, Kaang BK, Zhuo M (2016) Synaptic plasticity in the anterior cingulate cortex in acute and chronic pain. *Nat Rev Neurosci* 17:485–496.
18. Upadhyay J, et al. (2011) Default-mode-like network activation in awake rodents. *PLoS One* 6:e27839.
19. Logothetis NK (2003) The underpinnings of the BOLD functional magnetic resonance imaging signal. *J Neurosci* 23:3963–3971.
20. Rauch A, Rainer G, Augath M, Oeltermann A, Logothetis NK (2008) Pharmacological MRI combined with electrophysiology in non-human primates: Effects of lidocaine on primary visual cortex. *Neuroimage* 40:590–600.
21. Miller KJ, Weaver KE, Ojemann JG (2009) Direct electrophysiological measurement of human default network areas. *Proc Natl Acad Sci USA* 106:12174–12177.
22. Dastjerdi M, et al. (2011) Differential electrophysiological response during rest, self-referential, and non-self-referential tasks in human posteromedial cortex. *Proc Natl Acad Sci USA* 108:3023–3028.
23. Ossandón T, et al. (2011) Transient suppression of broadband gamma power in the default-mode network is correlated with task complexity and subject performance. *J Neurosci* 31:14521–14530.
24. Ramot M, et al. (2012) A widely distributed spectral signature of task-negative electrocorticography responses revealed during a visuomotor task in the human cortex. *J Neurosci* 32:10458–10469.
25. Kojima T, et al. (2009) Default mode of brain activity demonstrated by positron emission tomography imaging in awake monkeys: Higher rest-related than working memory-related activity in medial cortical areas. *J Neurosci* 29:14463–14471.
26. Mantini D, et al. (2011) Default mode of brain function in monkeys. *J Neurosci* 31:12954–12962.
27. Bentley WJ, Li JM, Snyder AZ, Raichle ME, Snyder LH (2016) Oxygen level and LFP in task-positive and task-negative areas: Bridging BOLD fMRI and electrophysiology. *Cereb Cortex* 26:346–357.
28. Hayden BY, Smith DV, Platt ML (2009) Electrophysiological correlates of default-mode processing in macaque posterior cingulate cortex. *Proc Natl Acad Sci USA* 106:5948–5953.
29. Pearson JM, Heilbronner SR, Barack DL, Hayden BY, Platt ML (2011) Posterior cingulate cortex: Adapting behavior to a changing world. *Trends Cogn Sci* 15:143–151.
30. Popa D, Popescu AT, Paré D (2009) Contrasting activity profile of two distributed cortical networks as a function of attentional demands. *J Neurosci* 29:1191–1201.
31. Nair J, et al. (2016) Gamma band directional interactions between basal forebrain and visual cortex during wake and sleep states. *J Physiol Paris* 110:19–28.
32. Zaborszky L, et al. (2015) Neurons in the basal forebrain project to the cortex in a complex topographic organization that reflects corticocortical connectivity patterns: An experimental study based on retrograde tracing and 3D reconstruction. *Cereb Cortex* 25:118–137.
33. Chandler DJ, Lamperski CS, Waterhouse BD (2013) Identification and distribution of projections from monoaminergic and cholinergic nuclei to functionally differentiated subregions of prefrontal cortex. *Brain Res* 1522:38–58.
34. Bloem B, et al. (2014) Topographic mapping between basal forebrain cholinergic neurons and the medial prefrontal cortex in mice. *J Neurosci* 34:16234–16246.
35. Kim T, et al. (2015) Cortically projecting basal forebrain parvalbumin neurons regulate cortical gamma band oscillations. *Proc Natl Acad Sci USA* 112:3535–3540, and erratum (2015) 112:E2848.
36. Li CSR, et al. (2014) Resting state functional connectivity of the basal nucleus of Meynert in humans: In comparison to the ventral striatum and the effects of age. *Neuroimage* 97:321–332.
37. Harvey M, Lau D, Civillico E, Rudy B, Contreras D (2012) Impaired long-range synchronization of gamma oscillations in the neocortex of a mouse lacking Kv3.2 potassium channels. *J Neurophysiol* 108:827–833.
38. Barthó P, et al. (2004) Characterization of neocortical principal cells and interneurons by network interactions and extracellular features. *J Neurophysiol* 92:600–608.
39. Niell CM, Stryker MP (2010) Modulation of visual responses by behavioral state in mouse visual cortex. *Neuron* 65:472–479.
40. Williamson RS, Hancock KE, Shinn-Cunningham BG, Polley DB (2015) Locomotion and task demands differentially modulate thalamic audiovisual processing during active search. *Curr Biol* 25:1885–1891.
41. Deco G, Thiele A (2011) Cholinergic control of cortical network interactions enables feedback-mediated attentional modulation. *Eur J Neurosci* 34:146–157.
42. Marguet SL, Harris KD (2011) State-dependent representation of amplitude-modulated noise stimuli in rat auditory cortex. *J Neurosci* 31:6414–6420.
43. Hasselmo ME, Sarter M (2011) Modes and models of forebrain cholinergic neuromodulation of cognition. *Neuropsychopharmacology* 36:52–73.
44. Lin SC, Brown RE, Hussain Shuler MG, Petersen CC, Kepecs A (2015) Optogenetic dissection of the basal forebrain neuromodulatory control of cortical activation, plasticity, and cognition. *J Neurosci* 35:13896–13903.
45. Disney AA, Aoki C, Hawken MJ (2007) Gain modulation by nicotine in macaque v1. *Neuron* 56:701–713.
46. Disney AA, Aoki C, Hawken MJ (2012) Cholinergic suppression of visual responses in primate V1 is mediated by GABAergic inhibition. *J Neurophysiol* 108:1907–1923.
47. Shimegi S, et al. (2016) Cholinergic and serotonergic modulation of visual information processing in monkey V1. *J Physiol Paris* 110:44–51.
48. Soma S, Shimegi S, Suematsu N, Sato H (2013) Cholinergic modulation of response gain in the rat primary visual cortex. *Sci Rep* 3:1138.
49. Soma S, Shimegi S, Osaki H, Sato H (2012) Cholinergic modulation of response gain in the primary visual cortex of the macaque. *J Neurophysiol* 107:283–291.
50. Herrero JL, et al. (2008) Acetylcholine contributes through muscarinic receptors to attentional modulation in V1. *Nature* 454:1110–1114.
51. Kang JI, Vaucher E (2009) Cholinergic pairing with visual activation results in long-term enhancement of visual evoked potentials. *PLoS One* 4:e5995.
52. Dotigny F, Ben Amor AY, Burke M, Vaucher E (2008) Neuromodulatory role of acetylcholine in visually-induced cortical activation: Behavioral and neuroanatomical correlates. *Neuroscience* 154:1607–1618.
53. Goard M, Dan Y (2009) Basal forebrain activation enhances cortical coding of natural scenes. *Nat Neurosci* 12:1444–1449.
54. Pinto L, et al. (2013) Fast modulation of visual perception by basal forebrain cholinergic neurons. *Nat Neurosci* 16:1857–1863.
55. De Luna P, Veit J, Rainer G (2017) Basal forebrain activation enhances between-trial reliability of low-frequency local field potentials (LFP) and spiking activity in tree shrew primary visual cortex (V1). *Brain Struct Funct* 222:4239–4252.
56. Quinn LK, Nitz DA, Chiba AA (2010) Learning-dependent dynamics of beta-frequency oscillations in the basal forebrain of rats. *Eur J Neurosci* 32:1507–1515.
57. Hangya B, Kepecs A (2015) Vision: How to train visual cortex to predict reward time. *Curr Biol* 25:R490–R492.
58. Gielow MR, Zaborszky L (2017) The input-output relationship of the cholinergic basal forebrain. *Cell Rep* 18:1817–1830.
59. Do JP, et al. (2016) Cell type-specific long-range connections of basal forebrain circuit. *Elife* 5:e13214.
60. Yang C, McKenna JT, Brown RE (2017) Intrinsic membrane properties and cholinergic modulation of mouse basal forebrain glutamatergic neurons in vitro. *Neuroscience* 352:249–261.
61. Xu M, et al. (2015) Basal forebrain circuit for sleep-wake control. *Nat Neurosci* 18:1641–1647.
62. van der Meer MA, et al. (2010) Integrating early results on ventral striatal gamma oscillations in the rat. *Front Neurosci* 4:300.
63. Kalenscher T, Lansink CS, Lankelma JV, Pennartz CM (2010) Reward-associated gamma oscillations in ventral striatum are regionally differentiated and modulate local firing activity. *J Neurophysiol* 103:1658–1672.
64. Malhotra S, Cross RW, Zhang A, van der Meer MA (2015) Ventral striatal gamma oscillations are highly variable from trial to trial, and are dominated by behavioural state, and only weakly influenced by outcome value. *Eur J Neurosci* 42:2818–2832.
65. Yang C, et al. (2014) Cholinergic neurons excite cortically projecting basal forebrain GABAergic neurons. *J Neurosci* 34:2832–2844.
66. Chen Z, Resnik E, McFarland JM, Sakmann B, Mehta MR (2011) Speed controls the amplitude and timing of the hippocampal gamma rhythm. *PLoS One* 6:e21408.
67. Berke JD (2009) Fast oscillations in cortical-striatal networks switch frequency following rewarding events and stimulant drugs. *Eur J Neurosci* 30:848–859.
68. Berke JD, Okatan M, Skurski J, Eichenbaum HB (2004) Oscillatory entrainment of striatal neurons in freely moving rats. *Neuron* 43:883–896.
69. van der Meer MA, Redish AD (2009) Low and high gamma oscillations in rat ventral striatum have distinct relationships to behavior, reward, and spiking activity on a learned spatial decision task. *Front Integr Neurosci* 3:9.
70. Howe MW, Atallah HE, McCool A, Gibson DJ, Graybiel AM (2011) Habit learning is associated with major shifts in frequencies of oscillatory activity and synchronized spike firing in striatum. *Proc Natl Acad Sci USA* 108:16801–16806.
71. Buzsáki G, Wang XJ (2012) Mechanisms of gamma oscillations. *Annu Rev Neurosci* 35:203–225.
72. Fries P (2005) A mechanism for cognitive dynamics: Neuronal communication through neuronal coherence. *Trends Cogn Sci* 9:474–480.
73. Lima B, Singer W, Neuenschwander S (2011) Gamma responses correlate with temporal expectation in monkey primary visual cortex. *J Neurosci* 31:15919–15931.
74. Vinck M, et al. (2010) Gamma-phase shifting in awake monkey visual cortex. *J Neurosci* 30:1250–1257.
75. Ray S, Maunsell JH (2015) Do gamma oscillations play a role in cerebral cortex? *Trends Cogn Sci* 19:78–85.
76. Wishaw IQ, O'Connor WT, Dunnett SB (1985) Disruption of central cholinergic systems in the rat by basal forebrain lesions or atropine: Effects on feeding, sensorimotor behaviour, locomotor activity and spatial navigation. *Behav Brain Res* 17:103–115.
77. Kalueff AV, et al. (2016) Neurobiology of rodent self-grooming and its value for translational neuroscience. *Nat Rev Neurosci* 17:45–59.